



Discovery of N-substituted-3-phenyl-1,6-naphthyridinone derivatives bearing quinoline moiety as selective type II c-Met kinase inhibitors against VEGFR-2

Hongchuang Xu¹, Minshu Wang¹, Fengxu Wu¹, Linsheng Zhuo*, Wei Huang*, Nengfang She*

Key Laboratory of Pesticide & Chemical Biology of Ministry of Education, International Joint Research Center for Intelligent Biosensor Technology and Health, College of Chemistry, Central China Normal University, Wuhan 430079, China

ARTICLE INFO

Keywords:

c-Met kinase inhibitor
1,6-Naphthyridone
VEGFR-2 selectivity
Antitumor efficacy

ABSTRACT

New N-substituted-3-phenyl-1,6-naphthyridinone derivatives are designed and synthesized, based on structural modification of our previously reported compound **3**. Extensive enzyme-based SAR studies and PK evaluation led to the discovery of compound **4r**, with comparable c-Met potency to that of Cabozantinib and high VEGFR-2 selectivity, while Cabozantinib displayed no VEGFR-2 selectivity. More importantly, at oral doses of 45 mg/kg (Q.D.), compound **4r** exhibits significant tumor growth inhibition (93%) in a U-87MG human glioblastoma xenograft model. The promising selectivity against VEGFR-2 and excellent tumor growth inhibition of compound **4r** suggest that it could be used as a new lead molecule for further discovery of selective type II c-Met inhibitors.

1. Introduction

The receptor tyrosine kinase c-Met, also known as hepatocyte growth factor receptor (HGFR), which is encoded by c-Met proto-oncogene, has a high affinity for its naturally occurring ligand HGF (also known as scatter factor).^{1–3} Once combined with HGF, the c-Met can be activated and lead to the recruitment, phosphorylation, and activation of multiple downstream signaling cascades, resulting in cell proliferation, survival, motility, induction of cell polarity, scattering, angiogenesis, and invasion.^{3–5} Although the HGF/c-Met signaling pathways are essential for embryogenesis and tissue injury repair, dysregulation of the HGF/c-Met signaling pathway caused by c-Met protein over-expression, gene amplification or rearrangement, and transcriptional regulation, as well as autocrine or paracrine ligand stimulation, has been correlated with the promotion of multiple tumorigenic processes and poor prognoses.^{6–10} Thus, the c-Met protein has been determined as an important therapeutic target for cancer therapy.

Numerous small-molecule c-Met kinase inhibitors have been developed. According to their binding mode in the c-Met kinase domain, these inhibitors can be divided into two classes, known as type I and type II, which are typified by Capmatinib and Cabozantinib, respectively (see Fig. 1).^{11–13} Type I inhibitors are ATP-competitive inhibitors which bind in a U-shaped conformation to the ATP-binding site at the pocket entrance, while type II inhibitors adopt an extended

conformation through interactions with DFG residues of the activation loop to enter an allosteric region (adjacent to the ATP binding site) which is only accessible in the inactive DFG-out conformation of the kinase.^{3,14,15} Owing to their different binding modes, type I inhibitors often have high selectivity against other kinases, while type II inhibitors are often multi-target inhibitors. Despite the high selectivity of type I inhibitors, drug resistance to certain mutations near the active site of c-Met remains a significant issue in subsequent clinical treatment. Hopefully, type II inhibitors may prove more effective against the mutations, due to their capability of binding to the ATP-binding site, as well as the allosteric site beyond the entrance of the active site of c-Met.^{16,17} However, the potential off-target effects of type II inhibitors on other protein kinases may cause significant clinical issues affecting patient's quality of life, such as VEGFR-2 related side effects.¹⁸ To date, few selective type II c-Met inhibitors have been reported. Therefore, developing novel type II c-Met inhibitors with increased selectivity over other protein kinases is a challenging, but meaningful, subject.

In light of our previous studies, the 2,7-naphthyridinone and 1,6-naphthyridine moieties can serve as a key pharmacophoric group (block C) to demonstrate c-Met inhibition, and the 2-fluoro-1,4-substituted phenyl linker (block B) was generally conservative in the reported inhibitors. Moreover, fine-regulation of the functionalizable N(1) amine group of the 1,6-naphthyridin-4(1H)-one moiety could lead to selectivity improvement.^{19,20} Meanwhile, the quinoline moiety has been

* Corresponding authors.

E-mail addresses: zhuolinsheng199010@126.com (L. Zhuo), weihuanguan@126.com (W. Huang), nfshe@mail.cnu.edu.cn (N. She).

¹ These authors contributed equally to this work.

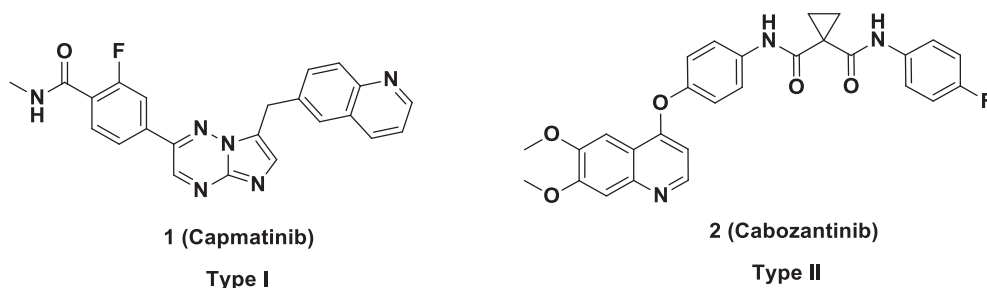


Fig. 1. Reported Type I and Type II c-Met inhibitors.

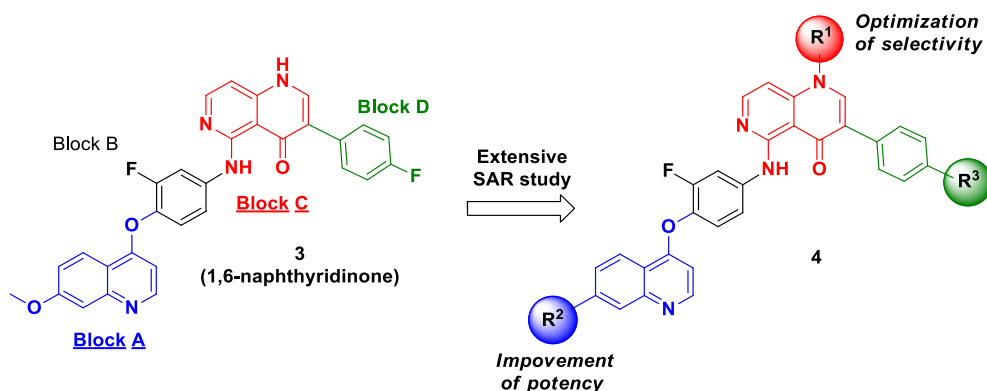


Fig. 2. Design of 1,6-naphthyridinone derivatives bearing a quinoline moiety in block A as new c-Met inhibitors.

proven to be a privileged scaffold in block A of type II c-Met inhibitors with favorable drug-like properties, such as Cabozantinib,¹³ TAS-115,²¹ Foretinib,²² RXDX-106,²³ AMG-458,²⁴ and Nintedanib.²⁵ Optimization of the substituents in the quinoline fragment could also improve potency.^{19,21} Therefore, our reported 1,6-naphthyridone-based c-Met kinase inhibitor **3**²⁶ bearing a quinoline moiety in block A, which displayed moderate c-Met potency but no VEGFR-2 selectivity, was selected as our starting point for this research, in order to improve its potency and selectivity (Fig. 2). In this paper, we describe our efforts to introduce structural modifications on the 1,6-naphthyridin-4(1H)-one and quinolone moieties, as well as on the terminal phenyl ring. A series of *N*-substituted-3-phenyl-1,6-naphthyridinone derivatives were prepared and all synthesized compounds were evaluated for their enzyme-based c-Met inhibition activity and VEGFR-2 selectivity. The most potent compound **4r** with high VEGFR-2 selectivity was also assessed for tumor growth inhibition in the U-87 MG xenograft model.

2. Result and discussion

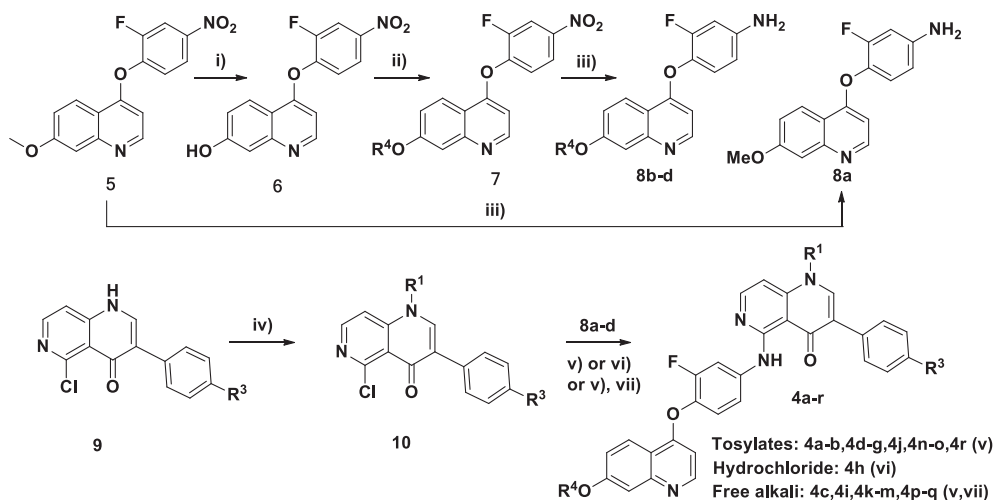
2.1. Chemistry

The designed compounds **4a–r** were synthesized following the general synthetic route illustrated in Scheme 1. Based on our previous study,²⁰ chlorinated 1,6-naphthyridone and aromatic amine were designed as two important synthetic building blocks. All compounds could be synthesized, in a modular fashion, by using aromatic nucleophilic substitution to join elaborated chlorinated 1,6-naphthyridone and aromatic amine. The aromatic amine building blocks were obtained using three steps, starting from our reported material **5**.^{24,27} The demethylation of starting material **5** yielded 4-(2-fluoro-4-nitrophenoxy)quinolin-7-ol **6**. Then, a subsequent substitution reaction of intermediate **6** with different halides or substituted oxiranes under a K_2CO_3 /DMF system generated the O-substituted intermediate **7**. Finally, reduction of the intermediates **7** using iron powder produced the key building blocks **8b–8d**; the key building block **8a** could be easily obtained by the direct reduction of the starting material **5**. The 1,6-

naphthyridone building blocks were also synthesized from our reported 1,6-naphthyridone block through substitution reactions with different halides or substituted oxiranes. Eventually, the target compounds were prepared via an acid-catalyzed aromatic nucleophilic substitution of the 5-Cl group of 1,6-naphthyridone **10a–k** with the aromatic amines **8a–d**.

2.2. In vitro biochemical c-Met/VEGFR-2 kinase inhibition activities

With the purpose to improve selectivity and potency, the primary goal of our initial investigation efforts was to validate whether functionalization of the N(1)–R¹ group of the 1,6-naphthyridin-4(1H)-one moiety could be tolerated for c-Met potency. Therefore, we initially designed methyl (**4a**), ethyl (**4b**), isopropyl (**4c**), 2-methoxyethyl (**4d**), and 2-methylpropan-2-ol (**4e**) substituents while keeping the OR⁴ and R³ groups as methoxy and fluorine, respectively. As expected, compounds **4a–e** all displayed comparable c-Met inhibitory activities to that of compound **3**, suggesting that substitution onto the N(1)–R¹ group could be tolerated for c-Met potency; more importantly, a breakthrough level in VEGFR-2 selectivity ($IC_{50,VEGFR-2} > 3000$ nM) was exhibited by all of these compounds, indicating that substitution on the N(1)–R¹ group could, indeed, improve VEGFR-2 selectivity. Encouraged by this, the 7-OR⁴ group was optimized immediately, hypothesizing that optimization of the 7-OR⁴ group could lead to the improvement of c-Met potency while retaining high VEGFR-2 selectivity. We were gratified to find that a consistent improvement of c-Met potency was observed by replacing the methoxy group with methoxyethyl (**4f**), alicyclic amines (**4g**), and 2-methylpropan-2-ol (**4h**) groups (see Table 1); where compound **4h** ($IC_{50} = 12.7$ nM, comparable to that of **2/Cabozantinib**) displayed a 3.3-fold increase in c-Met potency, compared to that of compound **3**, while maintaining high VEGFR-2 selectivity ($IC_{50,VEGFR-2} > 3000$ nM), indicating that the 2-methylpropan-2-ol group was the most suitable substituent for the 7-OR⁴ position. Due to the high c-Met potency and great selectivity profile against VEGFR-2 of compound **4h**, a more detailed SAR study of the N(1)–R¹ position was carried out, with the 2-methylpropan-2-ol group serving as an optimized 7-OR⁴ substituent. It was found that compound **4i**, possessing an ethyl substituent

**Table 1**

Activities of **4a-r** against c-Met and VEGFR-2 kinase^a and metabolic stability in human liver microsomes (HLMS).

Tosylates: 4a-b, 4d-g, 4j, 4n-o, 4r;
Hydrochloride: 4h;
Free alkali: 4c, 4i, 4k-m, 4p-q.

Compound	R ¹	R ² (OR ⁴)	R ³	IC ₅₀ , nM ^a		HLMS T _{1/2} , min
				c-Met	VEGFR-2	
4a	Me	OMe	F	32.5	> 3000	351.7
4b	Et	OMe	F	29.1	> 3000	–
4c	i-Pr	OMe	F	58.7	> 3000	–
4d		OMe	F	41.0	> 3000	–
4e		OMe	F	31.2	> 3000	–
4f	Me		F	35.6	> 3000	745.4
4g	Me		F	22.0	> 3000	257.2
4h	Me		F	12.7	> 3000	319.5
4i	Et		F	9.5	> 3000	164.8
4j	i-Pr		F	44.6	> 3000	–
4k			F	58.7	> 3000	–
4l			F	22.4	> 3000	–
4m			F	76.1	> 3000	–
4n			F	40.0	> 3000	–
4o			F	41.0	> 3000	–
4p	Bn		F	40.3	> 3000	–
4q			F	117.2	> 3000	–
4r	Me		H	10.6	> 3000	1061.8
2 (Cabozantinib)				8.4	7.0	–
3				41.4	71.1	–

^a In vitro kinase assays were performed with the indicated purified recombinant c-Met or VEGFR-2 kinase domains (nM).

at the N(1)-R¹ position, was as potent as compound **4h** (IC₅₀ of 9.5 nM, 1.3-fold to that of **4h**). Next, the sterically bulky substituents isopropyl (**4j**, IC₅₀ of 44.6 nM) and cyclopropylmethyl (**4k**, IC₅₀ of 58.7 nM) were introduced, consistent losses of c-Met potency were observed (3.5-fold and 4.6-fold compared with compound **4h**, respectively), suggesting that steric effects are the main cause for the slight loss of c-Met potency. Interestingly, the introduction of an oxiran-2-ylmethyl group (**4l**, IC₅₀ of 22.4 nM) exhibited a 2.6-fold increase of c-Met potency, compared with compound **4k**; it is hypothesized that the introduction of the oxygen atom formed a new interaction with c-Met protein, positively protecting against the inhibitory activity as a result of steric effects.

However, the consistent introduction of a 2-methoxyethyl group (**4m**, IC₅₀ of 76.1 nM) resulted in a 3.4-fold loss of potency, compared with compound **4k**, and compound **4n** (the demethylation product of **4m**) exhibited a slight increase in potency, compared with compound **4m** (40.0 nM vs 76.1 nM, 2.0-fold). Compounds **4o** (IC₅₀ of 41.0 nM) and **4p** (IC₅₀ of 40.3 nM), bearing two sterically bulky substituents, displayed comparable potency to that of compounds **4n** and **3**. The morpholine-substituted derivative **4q** (IC₅₀ of 117.2 nM) showed a 9.2-fold loss of potency, compared to that of compound **4h**. Finally, compound **4r**, which was generated by replacing the terminal 4-fluorophenyl ring of **4h** with a phenyl ring, displayed a comparable inhibitory activity (IC₅₀ of 10.6 nM) to that of compound **4h**.

2.3. Molecular docking study

Molecular docking experiments were further performed to explain the selectivity of **4r** between c-Met and VEGFR-2. As shown in Fig. 3A, compound **4r** was located deep in the c-Met pocket, and since five key H-bond interactions were observed in the binding mode: the first was established between the carbonyl group in block C and residue Asp1222, the second was established between the amine group in block C and residue Asp1222, the third formed between the N atom in block C and residue Lys1110, the fourth formed between N atom in block A and Met1160, the fifth formed between hydroxyl group in block A and Tyr1159, **4r** displayed comparable c-Met enzymatic activity to that of **2**. As shown in Fig. 3B, compound **4r** was located deep in the VEGFR-2 pocket, only two key H-bond interactions were observed in the binding mode: one was established between the N atom in block C and Lys868, another formed between N atom in block A and Cys919. The deflection of block B of **4r** resulted in a disappearance of two H-bond interactions between block C of **4r** and the residue Asp1046. The VEGFR-2 allele amino acid of Tyr1159 in c-Met was Phe918, which led to a disappearance of the H-bond interaction between hydroxyl group in block A and Tyr1159. And, the distance between methyl group in block C and the residue Glu885 was just 2.8 Å, which led to a steric conflict. In terms of van der Waals interaction, the hydrophobic interactions of **4r** with Leu1157, Phe1134, and Phe1200 in c-Met were stronger than the allele residues Thr916, Ile892, and Cys1024 in VEGFR-2. Together, these results suggest that the differences of key residues in active pocket between c-Met and VEGFR-2 led to the selectivity of **4r**. As shown in Fig. 3D, compound **2** was located deep in the VEGFR-2 pocket, and three key H-bond interactions were observed in the binding mode: the first was established between the carbonyl group in block C and residue Asp1046, the second was established between the carbonyl group in block C and residue Lys868, the third formed between N atom in block A and Cys919. In terms of van der Waals interaction, the hydrophobic

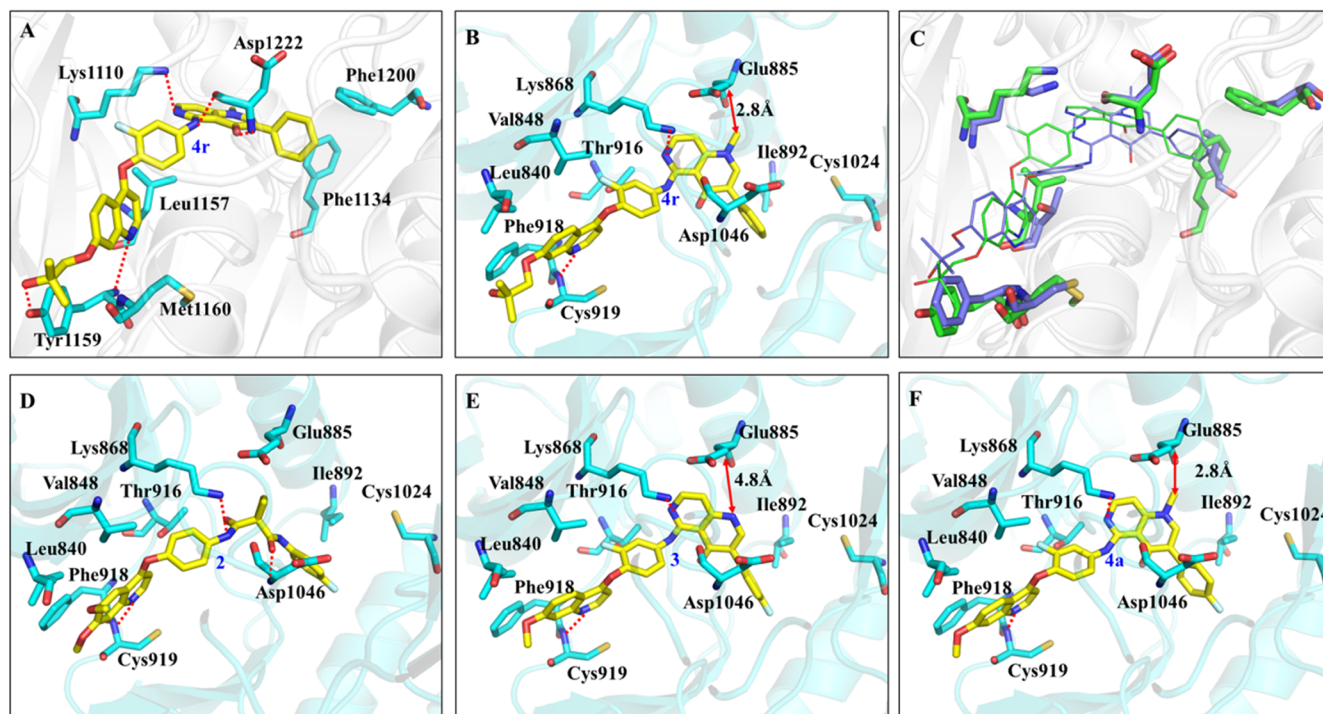


Fig. 3. (A) The proposed binding mode of **4r** with c-Met; (B) The proposed binding mode of **4r** with VEGFR-2; (C) The binding mode overlay of **4r** with c-Met (green) and **4r** with VEGFR-2 (light purple); (D) The proposed binding mode of **2** with VEGFR-2; (E) The proposed binding mode of **3** with VEGFR-2; (F) The proposed binding mode of **4a** with VEGFR-2. Each dashed red line represents hydrogen bonds between residues with **2**, **3**, **4a** or **4r**.

interactions of **2** with Val848, Leu840, Ile892 and Cys1024 were observed. Better binding efficiency of **2** displayed better VEGFR-2 enzymatic activity to that of **4r**. As shown in Fig. 3E and 3F, compounds **3** and **4a** were located deep in the VEGFR-2 pocket, two same key H-bond interactions were observed in the binding mode: one was established between the N atom in block C and Lys868, another formed between N atom in block A and Cys919. However, the distance between methyl group in block C of **4a** and the residue Glu885 was just 2.8 Å and was smaller than the distance between the N atom in block C of **3** and Glu885 4.8 Å, which led to a steric conflict. Therefore, these results suggest that the steric conflict of between methyl group and the residue Glu885 in active pocket of VEGFR-2 led to the selectivity of **4a**.

2.4. In vitro kinase activity profiling

The inhibitory activity of compound **4r** against a panel of other forty five kinases was also assayed. As shown in Fig. 4, compound **4r** only displayed high inhibitory effects (inhibition rate > 80% in 1 μM) against AXL, Mer and TYRO3 kinases. These kinase profiling data suggested that compound **4r** could be used a novel scaffold for further kinase selectivity enhancement.

2.5. In vitro antiproliferative activity

Antiproliferative activities of the selected compounds against three c-Met dependent cancer cell lines including U-87 MG (human glioblastoma), NIH-H460 (human lung cancer), and MKN-45 (human gastric cancer) were also evaluated in vitro using compound **2** (Cabozantinib) as a positive control. As shown in Table 2, compound **4h** showed only moderate to weak antiproliferative activity. Compound **4r** displayed good and broad-spectrum antiproliferative activity (IC₅₀ of 3.4–15.9 μM) against the tested three cancer cell lines, which is comparable to or slightly less active than compound **2** (Cabozantinib, IC₅₀ of 4.3–6.7 μM) (see Table 2).

2.6. In vitro and in vivo PK study

In order to evaluate the in vivo pharmacokinetic (PK) profiles of the highly potent compounds **4h** and **4r** quickly and efficiently, the PK properties of **4h** were first determined in a rat model. To our delight, compound **4h** displayed favorable overall PK profiles after oral dose (see Table 3), with a long half-life (8.1 h), moderate maximal plasma concentration (C_{max} = 0.8 μg/ml), high plasma exposure (AUC_{0-∞} = 10.1 h*μg/mL), favorable total clearance (CL = 0.5 l/h/kg), and

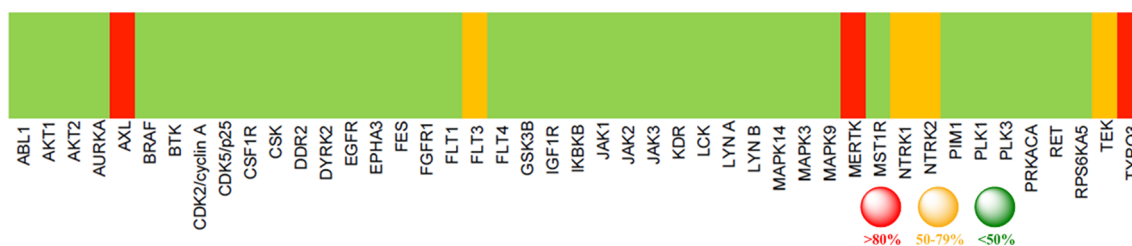


Fig. 4. Preliminary results of kinase activity profiling of **4r** (Inhibitory rate in 1 μM).

Table 2
Antiproliferative activities of selected compounds against U-87 MG, NIH-H460, and MKN-45 cell lines.

Compound	IC ₅₀ (μM)		
	U-87MG	NIH-H460	MKN-45
4h	22.9	35% ^a	29% ^a
4r	3.4	13.1	15.9
2	4.3	6.7	5.8

^a Inhibition rate at 50 μM.

moderate oral bioavailability (22%). Then, human liver microsomes stability experiments were conducted, in order to reasonably forecast the in vivo PK profiles of compounds **4h** and **4r** in human. Gratifyingly, compound **4r** displayed a 3.3-fold longer half-life in the human liver microsomes ($T_{1/2}$ = 1061.8 min), compared with compound **4h** ($T_{1/2}$ = 319.5 min). Moreover, compounds **4a**, **4g** and **4i** also displayed a moderate half-life ($T_{1/2}$ of 164.8 to 351.7 min), while compound **4f** ($T_{1/2}$ of 164.8 to 351.7 min) was very stable in human liver microsomes ($T_{1/2}$ of 745.4 min).

2.7. In vivo antitumor efficacy assessment

On the basis of the prominent enzymatic inhibitory activities and predictable favorable pharmacokinetic profiles, compound **4r** was selected for investigation of in vivo antitumor efficacy in the U-87 MG human glioblastoma xenograft model (Table 4 and Fig. 5). It was very exciting for us to find that compound **4r**, at oral doses of 45 mg/kg (Q.D.) for 21 days, could significantly inhibit tumor growth by 93% (TGI, $p < 0.001$); furthermore, partial tumor regression in two animals (PR 2/6) were observed. There was no significant effect of **4r** on the weight change of animals.

3. Conclusion

In summary, a series of *N*-substituted-3-phenyl-1,6-naphthyridinone derivatives was designed, based on the structural modification of our previously reported compound **3**, in order to improve c-Met potency and VEGFR-2 selectivity. Extensive enzyme-based SAR studies and in vivo PK evaluation led to the discovery of compound **4r**, which showed high VEGFR-2 selectivity and comparable c-Met potency to that of Cabozantinib, while Cabozantinib displayed no VEGFR-2 selectivity. More importantly, at oral doses of 45 mg/kg (Q.D.), compound **4r** exhibited significant tumor growth inhibition (93%) in a U-87MG human glioblastoma xenograft model. Due to its combination of promising selectivity against VEGFR-2 and excellent in vivo antitumor efficacy, compound **4r** could be used as a new lead molecule for the further research of selective type II c-Met inhibitors.

Table 3
In vivo PK profiles of compound **4h** in rat.^{a,b}

Compound	Route	Dose mg/kg	$T_{1/2}$ h	C_{max} μg/ml	AUC _{0-t} h*μg/ml	AUC _{0-∞} h*μg/ml	V _z L/kg	CL L/h/kg	T_{max} h	F %
4h	i.v.	1	8.3	2.3	9.0	9.2	1.3	0.1	–	–
	i.g.	5	8.1	0.8	9.6	10.1	6.2	0.5	2.7	22

^a Vehicle: 70% PEG400, 30% water. C_{max} , maximum concentration; T_{max} , time of maximum concentration; $T_{1/2}$, half-life; AUC_{0-∞}, area under the plasma concentration time curve; CL, clearance; V_z , volume of distribution; F, oral bioavailability.

^b Data reported as the average of three animals.

4. Experimental

4.1. Chemistry

Unless otherwise noted, all chemical reagents were commercially available and treated with standard methods. Silica gel column chromatography (CC). Silica gel (200–400 Mesh; Qingdao Makall Group Co., Ltd; Qingdao; China). Solvents were dried in a routine way and redistilled. All reactions involving air- or moisture-sensitive reagents were performed under a nitrogen or argon atmosphere. ¹H NMR spectra (400 MHz) and ¹³C NMR (100 MHz) spectra were recorded on a Bruker BioSpin AG (Ultrasield Plus AV 400) spectrometer as deuterium chloroform (CDCl₃) or dimethyl sulfoxide-*d*₆ (DMSO-*d*₆) solutions using tetramethyl silane (TMS) as an internal standard ($\delta = 0$) unless noted otherwise. ¹H NMR spectra (600 MHz) and ¹³C NMR (150 MHz) spectra were recorded on a Bruker BioSpin AG (Ultrasield Plus AV 600) spectrometer as deuterium chloroform (CDCl₃) or dimethyl sulfoxide-*d*₆ (DMSO-*d*₆) solutions using tetramethylsilane (TMS) as an internal standard ($\delta = 0$) unless noted otherwise. MS spectra were obtained on an Agilent technologies 6120 quadrupole LC/MS (ESI). All reactions were monitored using thin-layer chromatography (TLC) on silica gel plates. Yields were of purified compounds and were not optimized.

4.1.1. 5-((3-fluoro-4-((7-methoxyquinolin-4-yl)oxy)phenyl)amino)-3-(4-fluorophenyl)-1-methyl-1,6-naphthyridin-4(1H)-one 4-methylbenzenesulfonate (**4a**)

A solution of **10a** (0.5 mmol), **8a** (0.5 mmol) and PTSA (0.5 mmol) in isopropanol (10 mL) was heated to 90 °C under nitrogen for 2 h. The mixture was filtered, and the solid was washed with ice-cold ethanol to obtain **4a**. Yellow solid (83% yield). m.p.: 308–310 °C; ¹H NMR (600 MHz, DMSO-*d*₆) δ 13.62 (s, 1H), 9.02 (d, $J = 4.8$ Hz, 1H), 8.48 (d, $J = 8.4$ Hz, 1H), 8.42 (s, 1H), 8.26 (d, $J = 11.4$ Hz, 1H), 8.20 (d, $J = 3.6$ Hz, 1H), 7.81–7.58 (m, 2H), 7.69 (s, 1H), 7.63 (t, $J = 7.8$ Hz, 1H), 7.59 (d, $J = 8.4$ Hz, 1H), 7.55 (d, $J = 7.8$ Hz, 1H), 7.51 (d, $J = 6.6$ Hz, 2H), 7.33–7.25 (m, 2H), 7.19 (s, 1H), 7.12 (d, $J = 6.0$ Hz, 2H), 7.05 (s, 1H), 4.02 (s, 3H), 3.89 (s, 3H), 2.28 (s, 3H); ¹³C NMR (150 MHz, DMSO-*d*₆) δ 176.23, 166.60, 164.24, 162.42, 160.80, 155.07, 154.03, 152.39, 147.07, 146.66, 145.24, 144.38, 141.89, 138.02, 130.90, 130.34, 128.24, 125.53, 124.69, 124.18, 123.26, 121.82, 115.02, 114.88, 114.37, 107.12, 102.91, 102.15, 99.80, 56.51, 41.08, 20.86; ESI-MS m/z : 537.1 ([M+H]⁺).

4.1.2. 5-((3-fluoro-4-((7-methoxyquinolin-4-yl)oxy)phenyl)amino)-3-(4-fluorophenyl)-1-ethyl-1,6-naphthyridin-4(1H)-one 4-methylbenzenesulfonate (**4b**)

Prepared according to the procedure for the preparation of **4a**, from **10b** and **8a** to obtain **4b**. White solid (85% yield). m.p.: 195–197 °C; ¹H NMR (600 MHz, DMSO-*d*₆) δ 13.68 (s, 1H), 9.03 (d, $J = 6.6$ Hz, 1H), 8.54 (d, $J = 9.6$ Hz, 1H), 8.45 (s, 1H), 8.39 (d, $J = 12.0$ Hz, 1H), 8.25 (d, $J = 5.4$ Hz, 1H), 7.78 (d, $J = 5.4$ Hz, 1H), 7.76 (d, $J = 5.4$ Hz, 1H), 7.67–7.58 (m, 4H), 7.48 (d, $J = 7.8$ Hz, 2H), 7.31 (t, $J = 8.4$ Hz, 2H), 7.16 (d, $J = 6.6$ Hz, 1H), 7.14 (d, $J = 6.0$ Hz, 1H), 7.12 (d, $J = 7.8$ Hz,

Table 4
In vivo tumor growth inhibition activity in U-87 MG xenograft model.

Compound	Dose ^a (mg/kg)	TGI (%) ^b	PR ^c
4r	45	93**	2/6

^a 1Q.D. × 21, 70% PEG-400, H₂O, p.o.

^b TGI, Tumor growth inhibition value; **: P < 0.01.

^c PR, partial regression.

2H), 4.38 (q, *J* = 7.2 Hz, 2H), 4.04 (s, 3H), 2.29 (s, 3H), 1.40 (t, *J* = 7.2 Hz, 3H); ¹³C NMR (150 MHz, DMSO-*d*₆) δ 176.19, 166.50, 164.25, 162.56, 160.93, 154.76, 154.24, 152.60, 146.60, 144.97, 143.55, 141.85, 138.19, 137.06, 130.99, 130.95, 129.95, 128.29, 125.52, 124.64, 124.38, 121.88, 115.05, 114.91, 114.33, 107.38, 103.09, 102.04, 99.76, 56.54, 48.65, 20.85, 14.43; ESI-MS *m/z*: 551.6 ([M + H]⁺).

4.1.3. 5-((3-fluoro-4-((7-methoxyquinolin-4-yl)oxy)phenyl)amino)-3-(4-fluorophenyl)-1-isopropyl-1,6-naphthyridin-4(1H)-one (**4c**)

A solution of **10c** (0.5 mmol), **8a** (0.5 mmol) and PTSA (0.5 mmol) in isopropanol (10 mL) was heated to 90 °C under nitrogen for 2 h. The mixture was filtered, and the solid was washed with ice-cold ethanol. Then the solid was dissolved in ethyl acetate and stirred with DIPEA (1.0 mol) for 1 h at room temperature. The filtrate was concentrated in vacuum and purified by chromatography (Acetone/PE = 10:1) to obtain **4c**. White solid (85% yield). m.p.: 212–214 °C; ¹H NMR (600 MHz, DMSO-*d*₆) δ 13.60 (s, 1H), 8.60 (d, *J* = 4.8 Hz, 1H), 8.39 (d, *J* = 13.8 Hz, 1H), 8.28 (d, *J* = 5.4 Hz, 1H), 8.25–8.21 (m, 2H), 7.74–7.69 (m, 2H), 7.50 (d, *J* = 8.4 Hz, 1H), 7.43–7.37 (m, 2H), 7.31–7.23 (m, 3H), 7.20 (d, *J* = 6.0 Hz, 1H), 6.48 (d, *J* = 4.2 Hz, 1H), 5.04–4.97 (m, 1H), 3.93 (s, 3H), 1.51 (d, *J* = 6.0 Hz, 6H); ¹³C NMR (150 MHz, DMSO-*d*₆) δ 176.24, 162.33, 160.77, 156.45, 154.31, 152.68, 151.89, 151.20, 149.31, 146.24, 139.34, 137.82, 134.17, 131.21, 131.17, 130.99, 123.85, 123.49, 122.71, 118.88, 116.49, 114.81, 114.67, 114.63, 108.30, 107.38, 101.63, 100.67, 55.54, 51.45, 21.19; ESI-MS *m/z*: 565.4 ([M + H]⁺).

4.1.4. 5-((3-fluoro-4-((7-methoxyquinolin-4-yl)oxy)phenyl)amino)-3-(4-fluorophenyl)-1-(2-methoxyethyl)-1,6-naphthyridin-4(1H)-one 4-methylbenzenesulfonate (**4d**)

Prepared according to the procedure for the preparation of **4a**, from **10d** and **8a** to obtain **4d**. Yellow solid (80% yield). m.p.: 160–161 °C; ¹H NMR (600 MHz, DMSO-*d*₆) δ 13.64 (s, 1H), 9.02 (d, *J* = 6.6 Hz, 1H), 8.54 (d, *J* = 9.6 Hz, 1H), 8.42 (d, *J* = 12.0 Hz, 1H), 8.31 (s, 1H), 8.26 (d, *J* = 6.0 Hz, 1H), 7.74 (d, *J* = 5.4 Hz, 1H), 7.73 (d, *J* = 5.4 Hz, 1H),

7.67–7.59 (m, 4H), 7.48 (d, *J* = 7.8 Hz, 2H), 7.31 (t, *J* = 8.4 Hz, 2H), 7.19 (d, *J* = 6.0 Hz, 1H), 7.11 (d, *J* = 7.8 Hz, 3H), 4.55 (t, *J* = 4.8 Hz, 2H), 4.04 (s, 3H), 3.72 (t, *J* = 4.8 Hz, 2H), 3.26 (s, 3H), 2.28 (s, 3H); ¹³C NMR (150 MHz, DMSO-*d*₆) δ 176.26, 166.52, 164.24, 162.56, 160.93, 154.84, 154.20, 152.55, 147.12, 146.65, 144.99, 144.35, 141.86, 138.17, 130.93, 130.87, 129.95, 128.28, 125.53, 124.67, 124.54, 123.62, 121.86, 115.13, 114.99, 114.34, 107.33, 103.05, 102.33, 99.77, 69.68, 58.50, 56.49, 52.54, 20.84; ESI-MS *m/z*: 581.8 ([M + H]⁺).

4.1.5. 5-((3-fluoro-4-((7-methoxyquinolin-4-yl)oxy)phenyl)amino)-3-(4-fluorophenyl)-1-(2-hydroxy-2-methyl-propyl)-1,6-naphthyridin-4(1H)-one 4-methylbenzenesulfonate (**4e**)

Prepared according to the procedure for the preparation of **4a**, from **10e** and **8a** to obtain **4e**. Yellow solid (85% yield). m.p.: 231–233 °C; ¹H NMR (400 MHz, DMSO-*d*₆) δ 13.73 (s, 1H), 9.02 (d, *J* = 4.0 Hz, 1H), 8.54 (d, *J* = 7.6 Hz, 1H), 8.39 (d, *J* = 11.2 Hz, 1H), 8.29 (s, 1H), 8.18 (s, 1H), 7.79–7.57 (m, 6H), 7.48 (d, *J* = 5.6 Hz, 2H), 7.41–7.25 (m, 3H), 7.23–7.01 (m, 3H), 4.33 (s, 2H), 4.04 (s, 3H), 2.28 (s, 3H), 1.19 (s, 6H); ¹³C NMR (150 MHz, DMSO-*d*₆) δ 176.31, 166.50, 164.21, 162.54, 160.92, 154.64, 154.29, 152.65, 148.34, 146.50, 145.51, 145.13, 141.90, 138.08, 131.73, 130.88, 130.07, 128.26, 125.52, 124.65, 123.01, 121.87, 115.17, 115.03, 114.38, 107.27, 103.76, 103.18, 99.75, 70.35, 60.90, 56.49, 27.18, 20.86; ESI-MS *m/z*: 595.2 ([M + H]⁺).

4.1.6. 5-((3-fluoro-4-((7-(2-methoxyethoxy)quinolin-4-yl)oxy)phenyl)amino)-3-(4-fluorophenyl)-1-methyl-1,6-naphthyridin-4(1H)-one 4-methylbenzenesulfonate (**4f**)

Prepared according to the procedure for the preparation of **4a**, from **10a** and **8b** to obtain **4f**. White solid (70% yield). m.p.: 130–131 °C; ¹H NMR (600 MHz, DMSO-*d*₆) δ 13.62 (s, 1H), 9.01 (d, *J* = 6.6 Hz, 1H), 8.53 (d, *J* = 9.0 Hz, 1H), 8.46 (d, *J* = 12.6 Hz, 1H), 8.41 (s, 1H), 8.31 (d, *J* = 6.6 Hz, 1H), 7.75 (d, *J* = 6.0 Hz, 1H), 7.73 (d, *J* = 6.0 Hz, 1H), 7.66–7.57 (m, 4H), 7.48 (d, *J* = 7.8 Hz, 2H), 7.30 (t, *J* = 8.4 Hz, 2H), 7.11 (d, *J* = 7.8 Hz, 2H), 7.09 (d, *J* = 6.6 Hz, 1H), 7.04 (d, *J* = 6.6 Hz, 1H), 4.41–4.35 (m, 2H), 3.89 (s, 3H), 3.81–3.78 (m, 2H), 3.36 (s, 3H), 2.28 (s, 3H); ¹³C NMR (150 MHz, DMSO-*d*₆) δ 176.22, 166.59, 163.45, 162.44, 160.82, 154.97, 154.07, 152.42, 147.14, 146.74, 145.21, 144.40, 141.79, 138.04, 130.90, 130.29, 128.25, 125.53, 124.76, 124.25, 123.35, 121.87, 115.04, 114.90, 114.37, 107.12, 102.92, 102.20, 100.49, 69.93, 68.37, 58.34, 41.12, 20.86; ESI-MS *m/z*: 581.7 ([M + H]⁺).

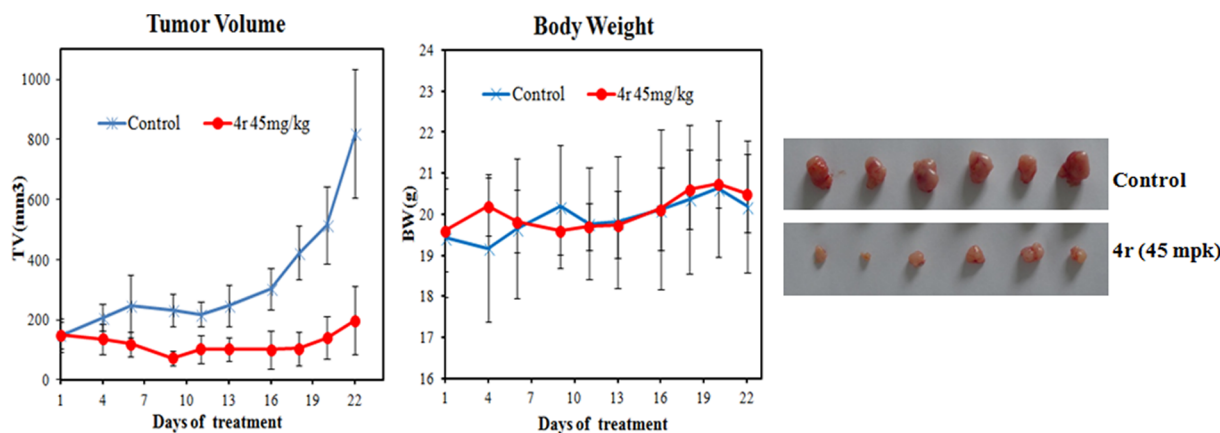


Fig. 5. Antitumor efficacy and body weight change of compound **4r** in the U-87 MG xenograft model. Tumor-bearing nude mice were randomly divided into groups when the tumor volume reached 100–200 mm³ and given compound **4r** p.o., at the indicated dose levels or vehicle alone, over the designated treatment schedule. Data are presented as mean ± SEM (n = 6 mice per group).

4.1.7. 5-((3-fluoro-4-((7-(3-morpholinopropoxy)quinolin-4-yl)oxy)phenyl)amino)-3-(4-fluorophenyl)-1-methyl-1,6-naphthyridin-4(1H)-one 4-methylbenzenesulfonate (**4g**)

Prepared according to the procedure for the preparation of **4a**, from **10a** and **8c** to obtain **4g**. Yellow solid (95% yield). m.p.: 190–192 °C; ¹H NMR (600 MHz, DMSO-*d*₆) δ 13.58 (s, 1H), 8.94 (d, *J* = 6.6 Hz, 1H), 8.54–8.47 (m, 2H), 8.39 (s, 1H), 8.33 (d, *J* = 5.4 Hz, 1H), 7.77–7.71 (m, 2H), 7.62 (d, *J* = 7.2 Hz, 2H), 7.58–7.52 (m, 2H), 7.48 (d, *J* = 7.2 Hz, 2H), 7.30 (t, *J* = 8.4 Hz, 2H), 7.11 (d, *J* = 7.2 Hz, 2H), 7.02 (d, *J* = 6.0 Hz, 1H), 6.96 (d, *J* = 5.4 Hz, 1H), 4.35 (t, *J* = 5.4 Hz, 2H), 4.04–3.97 (m, 2H), 3.88 (s, 3H), 3.82–3.74 (m, 2H), 3.54–3.48 (m, 4H), 3.43–3.36 (m, 2H), 3.17–3.07 (m, 2H), 2.35–2.29 (m, 2H), 2.28 (s, 3H); ¹³C NMR (150 MHz, DMSO-*d*₆) δ 176.27, 165.91, 162.67, 162.26, 160.65, 155.75, 153.80, 152.17, 148.82, 147.40, 146.51, 145.14, 144.01, 142.93, 140.16, 138.10, 130.79, 128.27, 125.53, 124.51, 123.64, 122.50, 121.28, 116.76, 114.90, 114.76, 114.46, 107.12, 102.57, 101.75, 101.58, 66.16, 63.32, 53.29, 51.20, 40.77, 22.82, 20.84; ESI-MS *m/z*: 649.7 ([M]⁺).

4.1.8. 5-((3-fluoro-4-((7-(2-hydroxy-2-methylpropoxy)quinolin-4-yl)oxy)phenyl)amino)-3-(4-fluorophenyl)-1-methyl-1,6-naphthyridin-4(1H)-one hydrochloride (**4h**)

A solution of **10a** (0.5 mmol), **8d** (0.5 mmol) and HCl (20 mmol%) in isopropanol (10 mL) was heated to 90 °C under nitrogen for 2 h. The mixture was filtered to obtain **4h**. Yellow solid (91% yield). m.p.: 168–169 °C; ¹H NMR (400 MHz, DMSO-*d*₆) δ 13.57 (s, 1H), 8.97 (d, *J* = 6.8 Hz, 1H), 8.50 (d, *J* = 9.2 Hz, 1H), 8.40 (s, 1H), 8.35 (d, *J* = 12.8 Hz, 1H), 8.23 (d, *J* = 6.4 Hz, 1H), 7.83–7.69 (m, 3H), 7.68–7.54 (m, 3H), 7.38–7.23 (m, 2H), 7.14 (d, *J* = 5.2 Hz, 1H), 7.04 (d, *J* = 6.4 Hz, 1H), 3.98 (s, 2H), 3.89 (s, 3H), 1.28 (s, 6H); ¹³C NMR (100 MHz, DMSO-*d*₆) δ 176.23, 162.18, 160.77, 160.56, 160.40, 155.85, 154.22, 152.59, 151.70, 150.97, 149.11, 146.43, 143.75, 139.23, 134.08, 130.79, 130.64, 123.79, 122.71, 122.42, 119.24, 119.02, 116.31, 114.86, 114.56, 108.45, 108.03, 107.02, 101.72, 101.47, 76.22, 68.59, 40.56, 26.61; ESI-MS *m/z*: 595.8 ([M+H]⁺).

4.1.9. 1-ethyl-5-((3-fluoro-4-((7-(2-hydroxy-2-methylpropoxy)quinolin-4-yl)oxy)phenyl)amino)-3-(4-fluoro-phenyl)-1,6-naphthyridin-4(1H)-one (**4i**)

Prepared according to the procedure for the preparation of **4c**, from **10b** and **8d** to obtain **4i**. Yellow solid (83% yield). m.p.: 202–203 °C; ¹H NMR (400 MHz, DMSO-*d*₆) δ 13.47 (s, 1H), 8.58 (d, *J* = 5.2 Hz, 1H), 8.37 (dd, *J* = 13.6, 2.0 Hz, 1H), 8.34 (s, 1H), 8.27 (d, *J* = 6.4 Hz, 1H), 8.22 (d, *J* = 9.0 Hz, 1H), 7.74 (d, *J* = 5.6 Hz, 1H), 7.72 (d, *J* = 5.6 Hz, 1H), 7.50 (d, *J* = 8.4 Hz, 1H), 7.41 (d, *J* = 9.0 Hz, 1H), 7.37 (d, *J* = 2.4 Hz, 1H), 7.32 (dd, *J* = 9.0, 2.4 Hz, 1H), 7.26 (t, *J* = 8.8, 8.8 Hz, 2H), 7.04 (d, *J* = 6.4 Hz, 1H), 6.48 (d, *J* = 5.2 Hz, 1H), 4.74 (s, 1H), 4.32 (q, *J* = 7.2 Hz, 2H), 3.91 (s, 2H), 1.39 (t, *J* = 7.2 Hz, 3H), 1.27 (s, 6H); ¹³C NMR (100 MHz, DMSO-*d*₆) δ 176.32, 162.61, 160.63, 160.35, 160.18, 156.25, 152.19, 151.77, 151.11, 149.18, 145.61, 142.83, 139.20, 134.27, 130.84, 130.76, 123.74, 122.96, 122.59, 119.08, 116.44, 114.78, 114.57, 108.44, 108.12, 107.37, 101.57, 101.09, 76.22, 68.54, 47.83, 26.57, 14.13; ESI-MS *m/z*: 608.6 ([M]⁺).

4.1.10. 5-((3-fluoro-4-((7-(2-hydroxy-2-methylpropoxy)quinolin-4-yl)oxy)phenyl)amino)-3-(4-fluorophenyl)-1-isopropyl-1,6-naphthyridin-4(1H)-one 4-methylbenzenesulfonate (**4j**)

Prepared according to the procedure for the preparation of **4a**, from **10c** and **8d** to obtain **4j**. White solid (74% yield). m.p.: 215–217 °C; ¹H NMR (400 MHz, DMSO-*d*₆) δ 13.56 (s, 1H), 8.58 (d, *J* = 5.2 Hz, 1H), 8.36 (dd, *J* = 13.6, 2.0 Hz, 1H), 8.26 (d, *J* = 6.4 Hz, 1H), 8.19–8.24 (m, 2H), 7.75–7.66 (m, 2H), 7.49 (d, *J* = 8.0 Hz, 1H), 7.43–7.34 (m, 2H), 7.31 (dd, *J* = 9.2, 2.2 Hz, 1H), 7.23–7.28 (m, 2H), 7.18 (d, *J* = 6.6 Hz, 1H), 6.47 (d, *J* = 5.0 Hz, 1H), 5.06–4.95 (m, 1H), 4.72 (s, 1H), 3.90 (s, 2H), 1.53 (d, *J* = 6.4 Hz, 6H), 1.27 (s, 6H); ¹³C NMR (100 MHz, DMSO-*d*₆) δ 176.20, 162.67, 160.65, 160.35, 160.24,

156.40, 154.63, 152.19, 151.77, 151.09, 149.25, 146.20, 139.24, 137.75, 134.26, 131.13, 131.05, 130.88, 123.73, 123.45, 122.59, 119.09, 116.47, 114.75, 114.54, 108.46, 108.23, 108.10, 107.31, 101.57, 100.61, 76.22, 68.54, 51.36, 26.57, 21.12; ESI-MS *m/z*: 623.7 ([M+H]⁺).

4.1.11. 1-(cyclopropylmethyl)-5-((3-fluoro-4-((7-(2-hydroxy-2-methylpropoxy)quinolin-4-yl)oxy)phenyl)amino)-3-(4-fluorophenyl)-1,6-naphthyridin-4(1H)-one (**4k**)

Prepared according to the procedure for the preparation of **4c**, from **10f** and **8d** to obtain **4k**. White solid (81% yield). m.p.: 194–195 °C; ¹H NMR (400 MHz, DMSO-*d*₆) δ 13.46 (s, 1H), 8.57 (d, *J* = 5.2 Hz, 1H), 8.40–8.32 (m, 2H), 8.26 (d, *J* = 6.0 Hz, 1H), 8.21 (d, *J* = 9.0 Hz, 1H), 7.71 (d, *J* = 5.6 Hz, 1H), 7.69 (d, *J* = 5.6 Hz, 1H), 7.50 (d, *J* = 8.4 Hz, 1H), 7.40 (d, *J* = 9.0 Hz, 1H), 7.36 (d, *J* = 2.0 Hz, 1H), 7.30 (dd, *J* = 9.2, 2.0 Hz, 1H), 7.20–7.28 (m, 2H), 7.13 (d, *J* = 6.4 Hz, 1H), 6.47 (d, *J* = 5.2 Hz, 1H), 4.71 (s, 1H), 4.17 (d, *J* = 6.8 Hz, 1H), 3.90 (s, 2H), 1.41–1.32 (m, 1H), 1.26 (s, 6H), 0.53–0.60 (m, 2H), 0.48–0.52 (m, 2H); ¹³C NMR (100 MHz, DMSO-*d*₆) δ 176.32, 162.62, 160.63, 160.34, 160.19, 156.18, 152.19, 151.77, 151.10, 149.13, 146.02, 142.87, 139.20, 134.27, 130.84, 130.69, 123.73, 122.78, 122.58, 119.08, 116.45, 114.81, 114.60, 108.45, 108.22, 108.12, 107.31, 101.57, 101.41, 76.22, 68.54, 56.27, 26.56, 10.34, 3.67; ESI-MS *m/z*: 635.6 ([M+H]⁺).

4.1.12. 5-((3-fluoro-4-((7-(2-hydroxy-2-methylpropoxy)quinolin-4-yl)oxy)phenyl)amino)-3-(4-fluorophenyl)-1-(oxiran-2-ylmethyl)-1,6-naphthyridin-4(1H)-one (**4l**)

Prepared according to the procedure for the preparation of **4c**, from **10g** and **8d** to obtain **4l**. Yellow solid (76% yield). m.p.: 234–235 °C; ¹H NMR (400 MHz, CDCl₃) δ 13.14 (s, 1H), 8.55 (d, *J* = 5.2 Hz, 1H), 8.34–8.16 (m, 3H), 7.56 (s, 1H), 7.54 (d, *J* = 5.6 Hz, 1H), 7.52 (d, *J* = 5.6 Hz, 1H), 7.46–7.40 (m, 1H), 7.38 (d, *J* = 2.4 Hz, 1H), 7.28–7.21 (m, 2H), 7.20–7.14 (m, 1H), 7.13–7.09 (m, 1H), 6.63 (d, *J* = 6.4 Hz, 1H), 6.44 (d, *J* = 5.2 Hz, 1H), 4.51 (dd, *J* = 15.6, 5.6 Hz, 1H), 4.03 (dd, *J* = 15.6, 5.6 Hz, 1H), 3.96 (s, 2H), 3.42–3.35 (m, 1H), 2.97–2.92 (m, 1H), 2.62–2.56 (m, 1H), 1.40 (s, 6H); ¹³C NMR (100 MHz, DMSO-*d*₆) δ 176.49, 162.67, 160.63, 160.35, 160.24, 156.06, 152.20, 151.78, 151.11, 149.22, 146.65, 143.53, 139.15, 134.49, 134.33, 130.82, 130.58, 123.75, 122.73, 122.59, 119.09, 116.50, 114.87, 114.66, 114.56, 108.51, 108.28, 107.15, 101.58, 76.22, 68.55, 53.29, 49.58, 44.87, 39.92, 26.57; ESI-MS *m/z*: 636.6 ([M]⁺).

4.1.13. 5-((3-fluoro-4-((7-(2-hydroxy-2-methylpropoxy)quinolin-4-yl)oxy)phenyl)amino)-3-(4-fluorophenyl)-1-(2-methoxyethyl)-1,6-naphthyridin-4(1H)-one (**4m**)

Prepared according to the procedure for the preparation of **4c**, from **10d** and **8d** to obtain **4m**. Yellow solid (86% yield). m.p.: 186–188 °C; ¹H NMR (400 MHz, DMSO-*d*₆) δ 13.44 (s, 1H), 8.59 (d, *J* = 5.2 Hz, 1H), 8.37 (dd, *J* = 13.6, 2.0 Hz, 1H), 8.26 (d, *J* = 6.0 Hz, 1H), 8.24–8.19 (m, 2H), 7.71 (d, *J* = 5.6 Hz, 1H), 7.69 (d, *J* = 6.0 Hz, 1H), 7.51 (dd, *J* = 9.2, 1.2 Hz, 1H), 7.41 (d, *J* = 9.0 Hz, 1H), 7.37 (d, *J* = 2.4 Hz, 1H), 7.31 (dd, *J* = 9.2, 2.4 Hz, 1H), 7.23–7.29 (m, 2H), 7.08 (d, *J* = 6.4 Hz, 1H), 6.48 (d, *J* = 5.2 Hz, 1H), 4.73 (s, 1H), 4.49 (t, *J* = 4.0, 4.0 Hz, 2H), 3.91 (s, 2H), 3.70 (t, *J* = 4.0, 4.0 Hz, 2H), 3.26 (s, 3H), 1.27 (s, 6H); ¹³C NMR (100 MHz, DMSO-*d*₆) δ 176.41, 160.64, 160.36, 160.21, 156.19, 151.80, 151.12, 149.10, 146.14, 143.80, 139.20, 134.31, 130.78, 130.70, 123.76, 122.61, 122.32, 119.10, 116.50, 114.89, 114.68, 114.56, 108.49, 108.13, 107.30, 101.60, 101.36, 76.22, 69.39, 68.55, 58.35, 51.93, 26.58; ESI-MS *m/z*: 636.7 ([M+H]⁺).

4.1.14. 5-((3-fluoro-4-((7-(2-hydroxy-2-methylpropoxy)quinolin-4-yl)oxy)phenyl)amino)-3-(4-fluorophenyl)-1-(2-hydroxyethyl)-1,6-naphthyridin-4(1H)-one 4-methylbenzenesulfonate (**4n**)

Prepared according to the procedure for the preparation of **4a**, from

10h and **8d** to obtain **4n**. White solid (80% yield). m.p.: 148–149 °C; ¹H NMR (400 MHz, DMSO-*d*₆) δ 13.65 (s, 1H), 8.99 (d, *J* = 6.4 Hz, 1H), 8.50 (d, *J* = 9.2 Hz, 1H), 8.37–8.26 (m, 2H), 8.16 (d, *J* = 6.4 Hz, 1H), 7.73 (d, *J* = 6.4 Hz, 1H), 7.71 (d, *J* = 5.6 Hz, 1H), 7.67 (s, 1H), 7.62 (d, *J* = 8.8 Hz, 2H), 7.59 (d, *J* = 4.8 Hz, 1H), 7.46 (d, *J* = 7.6 Hz, 2H), 7.32–7.23 (m, 2H), 7.19 (d, *J* = 6.4 Hz, 1H), 7.14 (d, *J* = 6.0 Hz, 1H), 7.08 (d, *J* = 7.6 Hz, 2H), 5.15 (br, 2H), 4.51–4.37 (m, 2H), 3.98 (s, 2H), 3.82–3.71 (m, 2H), 2.27 (s, 3H), 1.27 (s, 6H); ¹³C NMR (100 MHz, DMSO-*d*₆) δ 176.41, 160.64, 160.36, 160.21, 156.19, 151.80, 151.12, 149.11, 146.14, 143.80, 139.20, 134.32, 130.78, 130.67, 123.75, 122.60, 122.32, 119.10, 116.50, 114.89, 114.68, 114.57, 108.50, 108.14, 107.31, 101.60, 101.36, 76.23, 69.40, 68.56, 58.35, 51.93, 26.58; ESI-MS *m/z*: 625.6 ([M+H]⁺).

4.1.15. 5-((3-fluoro-4-((7-(2-hydroxy-2-methylpropoxy)quinolin-4-yl)oxy)phenyl)amino)-3-(4-fluorophenyl)-1-(2-hydroxy-2-methylpropyl)-1,6-naphthyridin-4(1H)-one 4-methylbenzene-sulfonate (4o)

Prepared according to the procedure for the preparation of **4a**, from **10e** and **8d** to obtain **4o**. White solid (78% yield). m.p.: 201–203 °C; ¹H NMR (600 MHz, DMSO-*d*₆) δ 13.75 (s, 1H), 9.02 (d, *J* = 6.6 Hz, 1H), 8.54 (d, *J* = 9.0 Hz, 1H), 8.34 (d, *J* = 12.6 Hz, 1H), 8.31 (s, 1H), 8.16 (d, *J* = 6.6 Hz, 1H), 7.75 (d, *J* = 6.0 Hz, 2H), 7.73 (d, *J* = 6.0 Hz, 1H), 7.70 (s, 1H), 7.68–7.58 (m, 3H), 7.48 (d, *J* = 7.8 Hz, 2H), 7.38 (d, *J* = 6.6 Hz, 1H), 7.32 (t, *J* = 8.4 Hz, 2H), 7.18 (d, *J* = 5.4 Hz, 1H), 7.12 (d, *J* = 7.8 Hz, 2H), 4.34 (s, 2H), 4.00 (s, 2H), 2.28 (s, 3H), 1.29 (s, 6H), 1.19 (s, 6H); ¹³C NMR (100 MHz, DMSO-*d*₆) δ 176.38, 166.53, 163.74, 162.76, 160.33, 155.44, 147.80, 146.63, 145.53, 145.22, 141.88, 137.68, 130.79, 130.71, 130.50, 128.06, 125.46, 124.68, 123.97, 121.89, 115.04, 114.83, 114.69, 114.32, 107.31, 103.40, 102.76, 102.59, 100.59, 76.86, 70.26, 68.48, 60.62, 27.19, 26.46, 20.76; ESI-MS *m/z*: 652.7 ([M]⁺).

4.1.16. 1-benzyl-5-((3-fluoro-4-((7-(2-hydroxy-2-methylpropoxy)quinolin-4-yl)oxy)phenyl)amino)-3-(4-fluorophenyl)-1,6-naphthyridin-4(1H)-one (4p)

Prepared according to the procedure for the preparation of **4c**, from **10i** and **8d** to obtain **4p**. Yellow solid (75% yield). m.p.: 198–199 °C; ¹H NMR (400 MHz, DMSO-*d*₆) δ 13.37 (s, 1H), 8.61–8.53 (m, 2H), 8.32 (d, *J* = 13.6 Hz, 1H), 8.21 (d, *J* = 9.0 Hz, 1H), 8.16 (d, *J* = 6.0 Hz, 1H), 7.80–7.71 (m, 2H), 7.49 (d, *J* = 8.0 Hz, 1H), 7.42–7.32 (m, 4H), 7.32–7.22 (m, 6H), 6.86 (d, *J* = 5.6 Hz, 1H), 6.46 (d, *J* = 5.6 Hz, 1H), 5.56 (s, 2H), 4.70 (s, 1H), 3.90 (s, 2H), 1.26 (s, 6H); ¹³C NMR (100 MHz, DMSO-*d*₆) δ 176.55, 162.68, 160.60, 160.34, 160.25, 156.10, 152.17, 151.77, 151.11, 149.19, 146.20, 143.69, 139.08, 135.82, 134.37, 130.95, 130.58, 128.84, 127.79, 126.51, 123.73, 123.06, 122.58, 119.09, 116.53, 114.86, 114.64, 114.56, 108.55, 108.12, 107.45, 101.79, 101.59, 76.21, 68.54, 55.50, 26.56; ESI-MS *m/z*: 671.7 ([M+H]⁺).

4.1.17. 5-((3-fluoro-4-((7-(2-hydroxy-2-methylpropoxy)quinolin-4-yl)oxy)phenyl)amino)-3-(4-fluorophenyl)-1-(2-morpholinoethyl)-1,6-naphthyridin-4(1H)-one (4q)

Prepared according to the procedure for the preparation of **4c**, from **10j** and **8d** to obtain **4q**. Yellow solid (79% yield). m.p.: 211–213 °C; ¹H NMR (600 MHz, DMSO-*d*₆) δ 13.49 (s, 1H), 8.59 (d, *J* = 4.8 Hz, 1H), 8.37 (d, *J* = 13.8 Hz, 1H), 8.26 (s, 2H), 8.22 (d, *J* = 9.0 Hz, 1H), 7.73–7.66 (m, 2H), 7.49 (d, *J* = 9.6 Hz, 1H), 7.42–7.35 (m, 2H), 7.33–7.26 (m, 3H), 7.03 (d, *J* = 4.8 Hz, 1H), 6.47 (d, *J* = 4.8 Hz, 1H), 4.78 (s, 1H), 4.37 (s, 2H), 3.89 (s, 2H), 3.52 (s, 4H), 2.66 (s, 2H), 2.46 (s, 4H), 1.25 (s, 6H); ¹³C NMR (150 MHz, CDCl₃) δ 176.33, 162.21, 160.67, 160.59, 160.36, 156.22, 154.25, 152.62, 151.14, 149.23, 145.86, 143.98, 139.22, 134.19, 130.85, 130.64, 123.86, 122.66, 122.14, 119.22, 116.44, 114.99, 114.85, 114.57, 108.19, 107.34, 101.66, 100.96, 76.22, 68.58, 66.33, 56.02, 53.26, 49.42, 26.61; ESI-MS *m/z*: 694.7 ([M+H]⁺).

4.1.18. 5-((3-fluoro-4-((7-(2-hydroxy-2-methylpropoxy)quinolin-4-yl)oxy)phenyl)amino)-1-methyl-3-phenyl-1,6-naphthyridin-4(1H)-one 4-methylbenzenesulfonate (4r)

Prepared according to the procedure for the preparation of **4a**, from **10k** and **8d** to obtain **4r**. Yellow solid (88% yield). m.p.: 179–181 °C; ¹H NMR (400 MHz, DMSO-*d*₆) δ 13.62 (s, 1H), 8.98 (d, *J* = 4.8 Hz, 1H), 8.51 (d, *J* = 8.8 Hz, 1H), 8.40 (d, *J* = 6.4 Hz, 1H), 8.37 (s, 1H), 8.25 (d, *J* = 4.4 Hz, 1H), 7.71–7.63 (m, 4H), 7.63–7.56 (m, 3H), 7.50–7.39 (m, 4H), 7.36 (d, *J* = 6.4 Hz, 1H), 7.09 (d, *J* = 6.4 Hz, 2H), 7.03 (d, *J* = 4.4 Hz, 1H), 3.99 (s, 2H), 3.89 (s, 3H), 2.28 (s, 3H), 1.28 (s, 6H); ¹³C NMR (100 MHz, DMSO-*d*₆) δ 176.34, 166.52, 163.72, 155.31, 154.29, 151.85, 146.94, 146.51, 145.44, 144.23, 141.82, 137.70, 134.08, 128.79, 128.04, 127.98, 127.39, 125.43, 124.64, 124.18, 123.93, 121.85, 114.29, 107.16, 102.71, 101.99, 100.54, 40.85, 26.43, 20.72; ESI-MS *m/z*: 577.5 ([M+H]⁺).

4.2. c-Met/VEGFR-2 enzymatic assay

The ability of compounds to inhibit the activity of two kinases (c-Met and VEGFR-2) was tested in vitro. Enzyme assays were run in homogeneous time-resolved fluorescence (HTRF) format in 384-well microtiter plates using purified kinases purchased from Invitrogen (Carlsbad, CA, US). The HTRF KinEASE TK kit (contains substrate-biotin, antibody-cryptate, streptavidin-XL665, 5 × enzymatic buffer, and detection buffer) was purchased from Cisbio (Codolet, France), and the kinase assays were performed according to the manufacturer's instructions. After the kinases and the compounds incubated at 25–30 °C for 5 min, the reactions were initiated by the addition of 2 μL of mixed substrate solution (mixed solution of ATP (Sigma, Shanghai, China) and substrate-biotin). The final concentrations of kinases were at EC₈₀ and the total reaction volume was 8 μL. Plates were incubated at 30 °C for 30–60 min, then the reactions were quenched by the addition 8 μL mixed detection solution (mixed solution of antibody-cryptate and streptavidin-XL665 in detection buffer). The fluorescence excitation wavelength was 320 nm. The fluorescence at 665 nm (acceptor emission wavelength) and 620 nm (donor emission wavelength) was measured with a PHERAstarFS plate reader (BMG, LABTECH, Ortenberg, Germany) using a time delay of 50 μs. All kinase assays were conducted using ATP concentrations below the enzyme *K*_{mapp} and kinase-specific biotinylated substrate peptides.

The data for dose responses were plotted as percentage of inhibition calculated with the data reduction formula $100 \times [1 - (U_1 - C_2)/(C_1 - C_2)]$ versus concentration of compound, where *U* is the emission ratio of 665 nm and 620 nm of test sample, *C*₁ is the average value obtained for solvent control (2% DMSO), and *C*₂ is the average value obtained for no reaction control (no kinase sample). Inhibition curves were generated by plotting percentage of control activity versus log₁₀ of the concentration of each kinase. The IC₅₀ values were calculated by nonlinear regression with Graphpad Prism 5 (GraphPad Software, San Diego, CA).

4.3. Molecular modeling

The three-dimensional structures of the small molecules were constructed and primarily optimized by Sybyl 2.0 software. Steepest descent and conjugate gradient methods were used in the optimization process. Autodock Tools was used to assign Gasteiger charges for both the receptors and inhibitors. The optimized probes were docked into the crystal structures of c-Met (PDB ID: 3F82) and VEGFR-2 (PDB ID: 3EFL) with Autodock 4.2.5, 1, respectively. The grid size was set to be 70 × 70 × 70 and the grid point spacing was set at default value 0.375 Å. A total of 256 runs were performed by using Lamarckian genetic algorithm (LGA) for conformational search. The best poses were selected for the binding model analysis for all the inhibitors. The figures were prepared with PyMOL 2.2.3.

4.4. Cell proliferation assay

Cells were seeded in 96-well tissue culture plates. On the next day, cells were exposed to various concentrations of compounds and further cultured for 72 h. Finally, cell proliferation was determined using thiazolyl blue tetrazolium bromide (MTT, Sigma) assay.

4.5. Pharmacokinetic profiles of compound 4h in SD rats

Compound 4h was dissolved in 70% PEG-400 solution and administered to 3 male SD rats (weight ranging from 180 g to 220 g) for i.v. and p.o. administration. The dosing volume was 2 mL/kg (i.v.) or 10 mL/kg (p.o.). After administration, blood samples were collected at the point including 5 min, 15 min, 30 min, 1 h, 2 h, 4 h, 6 h, 8 h, 10 h, 24 h, 48 h and 72 h (i.v.) or 15 min, 30 min, 45 min, 30 min, 1 h, 2 h, 4 h, 6 h, 8 h, 10 h, 24 h, 48 h and 72 h (p.o.) for analyses, the collected blood samples were centrifuged at 8000 rpm for 5 min at 4 °C, and then analyzed after protein precipitation. LC/MS/MS analysis of compound 4h was performed under optimized conditions to obtain the best sensitivity and selectivity of the analyte in selected reaction monitoring mode (SRM) containing an internal standard. Plasma concentration–time data were measured by a noncompartmental approach using the software Win Nonlin Enterprise, version 5.2 (Pharsight Co., Mountain View, CA).

4.6. In vivo antitumor efficacy of compound 4r in nude mice

Female nude mice (4–6 weeks old) were housed and maintained under specific-pathogen free conditions. Animal experiments were performed according to institutional ethical guidelines of animal care. Tumor cells were inoculated into the flanks of athymic nude mice (2×10^6 cells/mouse). When the tumor volume reached about 100–200 mm³, the mice were randomly assigned into control and treatment groups. Control groups were given vehicle alone, and treatment groups received synthesized compounds as indicated doses via p.o. administration 7 days per week for 3 weeks. The sizes of the tumors were measured three times per week using microcaliper. The tumour volume (V) was calculated as follows: $V = [\text{length (mm)} \times \text{width}^2 (\text{mm}^2)]/2$. Percent (%) inhibition values (TGI) were measured on the final day of study for drug-treated compared with vehicle-treated mice and were calculated as $100\% \times (1 - ((\text{treated}_{\text{final day}} - \text{treated}_{\text{day 0}})/\text{control}_{\text{final day}} - \text{control}_{\text{day 0}}))$. Significant differences between the treated versus the control groups ($P \leq 0.01$) were determined using Student's.

Declaration of Competing Interest

The authors declare that they have no known competing financial interests or personal relationships that could have appeared to influence the work reported in this paper.

Acknowledgments

This work was supported by the National Natural Science Foundation of China (No. 21272086), the Science and Technology Program of Wuhan, China (No. 2019020701011460), and the Fundamental Research Funds for the Central Universities (No. CCNU19QN073 & CCNU18TS009).

Appendix A. Supplementary material

Supplementary data to this article can be found online at <https://doi.org/10.1016/j.bmc.2020.115555>.

References

- Bottaro DP, Rubin JS, Faletto DL, et al. Identification of the hepatocyte growth factor receptor as the c-met proto-oncogene product. *Science*. 1991;251:802–804. <https://doi.org/10.1126/science.1846706>.
- Birchmeier C, Gherardi E. Developmental roles of HGF/SF and its receptor, the c-Met tyrosine kinase. *Trends Cell Biol*. 1998;8:404–410. [https://doi.org/10.1016/S0962-8924\(98\)01359-2](https://doi.org/10.1016/S0962-8924(98)01359-2).
- Parikh PK, Ghate MD. Recent advances in the discovery of small molecule c-Met Kinase inhibitors. *Eur J Med Chem*. 2018;143:1103–1138. <https://doi.org/10.1016/j.ejmech.2017.08.044>.
- Seiden-Long I, Navab R, Shih W, et al. Gab1 but not Grb2 mediates tumor progression in Met overexpressing colorectal cancer cells. *Carcinogenesis*. 2008;29:647–655. <https://doi.org/10.1093/carcin/bgn009>.
- Ma P, Tretiakova M, Nallasura V, et al. Downstream signalling and specific inhibition of c-MET/HGF pathway in small cell lung cancer: implications for tumour invasion. *Br J Cancer*. 2007;97:368–377. <https://doi.org/10.1038/sj.bjc.6603884>.
- Nakamura T, Mizuno S, Matsumoto K, et al. Myocardial protection from ischemia/reperfusion injury by endogenous and exogenous HGF. *J Clin Invest*. 2000;106:1511–1519. <https://doi.org/10.1172/JCI10226>.
- Li Y, Li W, He Q, et al. Prognostic value of MET protein overexpression and gene amplification in locoregionally advanced nasopharyngeal carcinoma. *Oncotarget*. 2015;6:13309–13319. <https://doi.org/10.18632/oncotarget.3751>.
- Liu L, Norman MH, Lee M, et al. Structure-based design of novel class II c-Met inhibitors: 2. SAR and kinase selectivity profiles of the pyrazolone series. *J Med Chem*. 2012;55:1868–1897. <https://doi.org/10.1021/jm201331s>.
- Birchmeier C, Birchmeier W, Gherardi E, et al. Met, metastasis, motility and more. *Nat Rev Mol Cell Biol*. 2003;4:915–925. <https://doi.org/10.1038/nrm1261>.
- Trusolino L, Comoglio PM. Scatter-factor and semaphorin receptors: cell signalling for invasive growth. *Nat Rev Cancer*. 2002;2:289–300. <https://doi.org/10.1038/nrn779>.
- Liu X, Wang Q, Yang G, et al. A novel kinase inhibitor, INCB28060, blocks c-MET-dependent signaling, neoplastic activities, and cross-talk with EGFR and HER-3. *Clin Cancer Res*. 2011;17:7127–7138. <https://doi.org/10.1158/1078-0432.CCR-11-1157>.
- Baltschukat S, Engstler BS, Huang A, et al. Capmatinib (INC280) is active against models of non-small cell lung cancer and other cancer types with defined mechanisms of MET activation. *Clin Cancer Res*. 2019;25:3164–3175. <https://doi.org/10.1158/1078-0432.CCR-18-2814>.
- U.S. Food and Drug Administration (Page Last Updated: 01/26/2017) <https://www.fda.gov/Drugs/DevelopmentApprovalProcess/DrugInnovation/ucm336115.htm>, last accessed 3 August 2017.
- Zhao S, Zhang F, Zhang W, et al. Determination of the solubility parameter of cellulose acrylate using inverse gas chromatography. *Chinese Sci Bull*. 2007;52:3051–3055. <https://doi.org/10.1007/s11434-007-0387-6>.
- Myers SH, Brunton VG, Unciti-Broceta A. AXL inhibitors in cancer: a medicinal chemistry perspective. *J Med Chem*. 2015;59:3593–3608. <https://doi.org/10.1021/acs.jmedchem.5b01273>.
- Dussault I, Bellon SF. c-Met inhibitors with different binding modes: two is better than one. *Cell Cycle*. 2008;7:1157–1160. <https://doi.org/10.4161/cc.7.9.5827>.
- Berthou S, Aebbersold DM, Schmidt LS, et al. The Met kinase inhibitor SU11274 exhibits a selective inhibition pattern toward different receptor mutated variants. *Oncogene*. 2004;23:5387–5393. <https://doi.org/10.1038/sj.onc.1207691>.
- D'Angelo ND, Bellon SF, Booker SK, et al. Design, synthesis, and biological evaluation of potent c-Met inhibitors. *J Med Chem*. 2008;51:5766–5779. <https://doi.org/10.1021/jm8006189>.
- Zhuo LS, Xu HC, Wang MS, et al. 2,7-naphthyridinone-based MET kinase inhibitors: a promising novel scaffold for antitumor drug development. *Eur J Med Chem*. 2019;178:705–714. <https://doi.org/10.1016/j.ejmech.2019.06.033>.
- Wang MS, Zhuo LS, Yang FP, et al. Synthesis and biological evaluation of new MET inhibitors with 1,6-naphthyridinone scaffold. *Eur J Med Chem*. 2020;185:111803–111816. <https://doi.org/10.1016/j.ejmech.2019.11.1803>.
- Fujita H, Miyadera K, Kato M, et al. The novel VEGF receptor/MET-targeted kinase inhibitor TAS-115 has marked in vivo antitumor properties and a favorable tolerability profile. *Mol Cancer Ther*. 2013;12:2685–2696. <https://doi.org/10.1158/1535-7163.mct-13-0459>.
- Zillhardt M, Park SM, Romero IL, et al. Foretinib (GSK1363089), an orally available multikinase inhibitor of c-Met and VEGFR-2, blocks proliferation, induces anoikis, and impairs ovarian cancer metastasis. *Clin Cancer Res*. 2011;17:4042–4051. <https://doi.org/10.1158/1078-0432.CCR-10-3387>.
- Yokoyama Y, Lew ED, Seelige R, et al. Immuno-oncological efficacy of RXDX-106, a novel TAM (TYRO3, AXL, MER) family small-molecule kinase inhibitor. *Cancer Res*. 2019;79:1996–2008. <https://doi.org/10.1158/0008-5472.CAN-18-2022>.
- Liu L, Siegmund A, Xi N, et al. Discovery of a potent, selective, and orally bioavailable c-Met Inhibitor: 1-(2-hydroxy-2-methylpropyl)-N-(5-(7-methoxyquinolin-4-yl)oxy)pyridin-2-yl)-5-methyl-3-oxo-2-phenyl-2,3-dihydro-1H-pyrazole-4-carboxamide (AMG 458). *J Med Chem*. 2008;51:3688–3691. <https://doi.org/10.1021/jm800401t>.
- Xi N, Zhang Y, Wang Z, et al. Abstract 1755: CT053PTSA, a novel c-MET and VEGFR2 inhibitor, potently suppresses angiogenesis and tumor growth. *Cancer Res*. 2014;74:1755. <https://doi.org/10.1158/1538-7445.AM2014-1755>.
- Huang W, Zhao XE, Cai JF, et al. Fused heterocyclic derivative and application thereof. WO2013097753A1, Jul 4, 2013.
- Xi N. Substituted quinolone compounds and methods of use. US20120219522, Aug 30, 2012.